Journal of Microscopy, Vol. 201, Pt 3, March 2001, pp. 395–403.
Received 11 August 2000; accepted 9 November 2000

High resolution protein localization using soft X-ray microscopy

W. MEYER-ILSE*[1], D. HAMAMOTO†, A. NAIR*, S. A. LELIÈVRE‡, G. DENBEAUX*, L. JOHNSON*, A. L. PEARSON*, D. YAGER‡, M. A. LEGROS* & C. A. LARABELL‡§

**Center for X-ray Optics, Lawrence Berkeley National Laboratory, 1 Cyclotron Road, Berkeley, CA 94720, U.S.A.*

†Advanced Light Source, Lawrence Berkeley National Laboratory, 1 Cyclotron Road, Berkeley, CA 94720, U.S.A.

‡Life Sciences Division, Lawrence Berkeley National Laboratory, 1 Cyclotron Road, Berkeley, CA 94720, U.S.A.

§Department of Anatomy, University of California, San Francisco, CA 94143, U.S.A.

Key words. Immunogold, protein localization, soft X-ray microscopy.

Summary

Soft X-ray microscopes can be used to examine whole, hydrated cells up to 10 μm thick and produce images approaching 30 nm resolution. Since cells are imaged in the X-ray transmissive 'water window', where organic material absorbs approximately an order of magnitude more strongly than water, chemical contrast enhancement agents are not required to view the distribution of cellular structures. Although living specimens cannot be examined, cells can be rapidly frozen at a precise moment in time and examined in a cryostage, revealing information that most closely approximates that in live cells. In this study, we used a transmission X-ray microscope at photon energies just below the oxygen edge ($\lambda = 2.4$ nm) to examine rapidly frozen mouse 3T3 cells and obtained excellent cellular morphology at better than 50 nm lateral resolution. These specimens are extremely stable, enabling multiple exposures with virtually no detectable damage to cell structures. We also show that silver-enhanced, immunogold labelling can be used to localize both cytoplasmic and nuclear proteins in whole, hydrated mammary epithelial cells at better than 50 nm resolution. The future use of X-ray tomography, along with improved zone plate lenses, will enable collection of better resolution (approaching 30 nm), three-dimensional information on the distribution of proteins in cells.

Correspondence to: Professor Carolyn A. Larabell, Lawrence Berkeley National Laboratory, 1 Cyclotron Road, MS 6-2100, Berkeley, CA 94720, U.S.A. Tel.: +1 510 486 5890; fax: +1 510 486 5664; e-mail: larabell@lbl.gov

[1]Werner Meyer-Ilse, who designed and built the X-ray microscope (XM-1) at LBNL, was tragically killed in a car accident on 14 July 1999.

Introduction

The imaging of cells using a variety of microscopes with distinctive capabilities has generated unique spatial and temporal information about cells and their responses to extracellular signals. Currently, the light microscope is the quintessential tool for monitoring the dynamics of live cells, whereas the transmission electron microscope (TEM) provides high-resolution information about the structural organization of cells that have been fixed at a precise moment in time. The use of light microscopy to track specific protein constructs tagged with green fluorescent protein (GFP) has facilitated studies of exogenous proteins in live cells (Lippincott-Schwartz *et al.*, 1998; Tsien, 1998; Lippincott-Schwartz *et al.*, 1999; Miller *et al.*, 1999; Larabell, 2000; Taunton *et al.*, 2000), and both light and TEM are being used to determine the location of endogenous proteins in fixed cells. Immunocytochemistry can be carried out in whole, hydrated cells using a light microscope; however, the spatial resolution attainable is often insufficient to answer questions regarding the precise location of proteins and protein complexes. The only available option until recently has been immunogold labelling and localization using TEM. Although TEM provides superb resolution, it requires extensive processing, including dehydration, embedding in plastic, and preparation of ultra thin sections (50–100 nm). These procedures are extremely time-consuming and can introduce artefacts and loss of antigenicity. An alternative approach for TEM immunocytochemistry, which better preserves the epitope, is immunogold labelling of glucose-treated frozen sections. This approach is generally successful but is extremely tedious and therefore infrequently used. There is a distinct need for a high-throughput approach that provides better resolution than light microscopy with minimal processing of the cells.

We show that soft X-ray microscopy, which achieves better than 50 nm resolution, can be used to localize proteins in whole, hydrated cells and can therefore bridge the existing gap between light and electron microscopy.

Soft X-ray microscopy has unique capabilities that make it a very useful tool for imaging cells (Kirz *et al.*, 1995; Schmahl *et al.*, 1996; Magowan *et al.*, 1997; Methe *et al.*, 1997; Jacobsen, 1999; Scharf & Schneider, 1999). The specimens are imaged in what is referred to as the 'water window', that is with X-rays with a range of photon energies between the K-shell absorption edges of carbon (284 eV) and oxygen (543 eV). In this energy range, organic matter absorbs approximately an order of magnitude more strongly than water. Operating at photon energies just below the oxygen edge, e.g. 517 eV (which corresponds to a wavelength of $\lambda = 2.4$ nm) enables examination of thick (up to 10 μm), hydrated cells. In this paper, we have used a conventional transmission X-ray microscope equipped with a zone plate condenser and objective (XM-1) (Meyer-Ilse *et al.*, 1995, 1999) located at the Advanced Light Source at Lawrence Berkeley National Laboratory (LBNL). Using this microscope, we have obtained high contrast images of whole, hydrated cells at better than 50 nm resolution. The use of a cryo-stage enabled examination of rapidly frozen cells that were not exposed to chemical fixatives or contrast enhancement agents and therefore more closely resemble their native state. As cells were examined using X-rays with 517 eV photon energy, where the 1/e attenuation lengths of water, organic material and silver are about 10 μm, 0.5 μm and 50 nm, respectively (Henke *et al.*, 1993), we can clearly distinguish dense, unlabelled cellular structures from silver-enhanced gold label. Consequently, we can use standard immunogold labelling techniques typically used for TEM and recently used to localize proteins in whole, dehydrated cells using dark-field X-ray microscopy with a scanning transmission X-ray microscope (Chapman *et al.*, 1996). Although chemical fixation is not required for X-ray microscopy of cryo-fixed specimens, it is required for immuocytochemistry and was used in the labelling work reported here. The future use of cryo X-ray microscopy to examine whole cells followed by tomography, as was recently demonstrated with the green alga *Chlamydomonas reinhardtii* (Weiss *et al.*, 2000) and cell monolayers (Wang *et al.*, 2000), will generate three-dimensional information about an entire cell and its organelles. This approach, when coupled with immunolabeling techniques, will yield unique, 3-D information about the distribution of proteins in whole, hydrated cells at unparalleled resolution.

Materials and methods

X-ray microscopy

The images shown here were collected using a conventional transmission X-ray microscope (XM-1) (Meyer-Ilse *et al.*, 1995, 1999). The specimen is fully hydrated and positioned between two thin (100 nm) low-absorption silicon nitride membranes then examined using photon energies just below the oxygen edge, i.e. 517 eV (corresponding to a wavelength of $\lambda = 2.4$ nm). Images were focused using Fresnel zone plates as the condenser and objective lenses. The spatial resolution is largely determined by the width of the outermost zone of the objective zone plate and is on the order of 30–45 nm, depending on the zone plate used, the sample contrast, and the attainable signal-to-noise ratio. The magnified image is recorded on a Peltier-cooled, back-illuminated, 1024 × 1024 soft X-ray CCD camera.

Zone plate lenses

The images were collected using a zone plate condenser lens to focus the synchrotron X-ray source on the sample and a zone plate objective lens to magnify and project the image onto the CCD. The condenser lenses are 9 mm in diameter, have an outermost zone width of 55 nm and a focal length of 205 mm at 517 eV photon energy (2.4 nm) [lenses produced by G. Schmahl and D. Rudolph, University of Göttingen (Schmahl *et al.*, 1996) or E. Anderson, Center for X-ray Optics, LBNL (Carter *et al.*, 1999)]. The objective zone plate lenses are 45 μm in diameter, have an outermost zone width of 35 nm, and a focal length of 650 μm at 517 eV photon energy (produced by E. Anderson, LBNL; Carter *et al.*, 1999). The resolution, using a knife-edge test, is 43 nm between 10% and 90% intensity (Heck *et al.*, 1998) (Figs 2–4) and 36 nm (Fig. 1). Additional information about these measurements is available at www.cxro.lbl.gov/microscopy.

Cryomicroscopy

Cells were cultured on 100 nm-thick silicon nitride support films, rinsed in phosphate-buffered saline (PBS), covered with another 100 nm-thick silicon nitride support film and placed on the microscope. They were then rapidly frozen by exposure to a jet of liquid nitrogen-cooled dry helium gas. This approach produces freezing rates on the order of 3000 °C s^{-1}, generating images virtually free of ice crystal artefacts at the level of resolution of the X-ray microscope (Meyer-Ilse *et al.*, 1999). Freezing rates of 3000 °C s^{-1} are not sufficient to achieve vitreous ice and well-frozen cells. Examination of the same cells using electron microscopy might reveal ice crystal damage that is undetectable at the level of resolution of the X-ray microscope configured with the zone plate used to obtain Fig. 1 (a zone plate with an outer zone width of 36 nm).

Immunocytochemistry

For localization of tubulin, cells were cultured on 100 nm thin silicon nitride support films, rinsed in PBS (37 °C), then

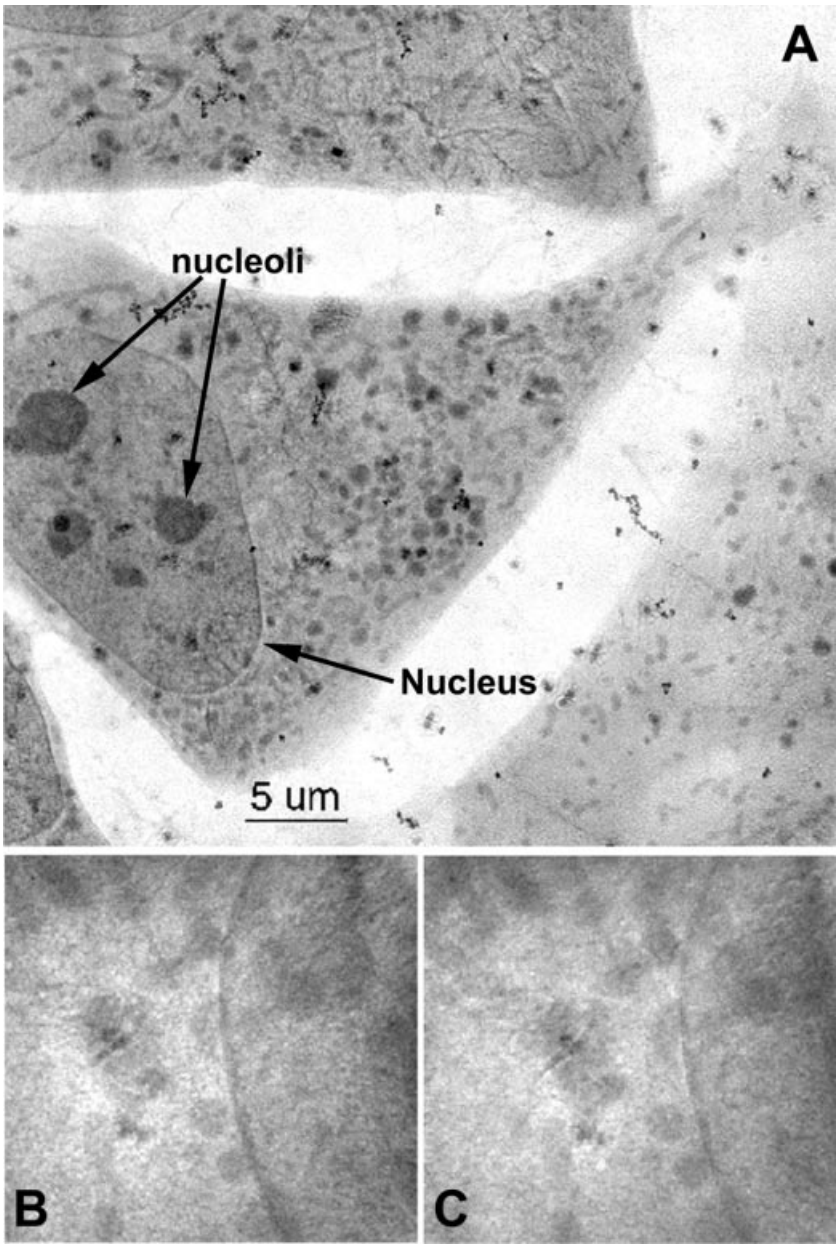

Fig. 1. Cryo X-ray microscopy of whole, hydrated 3T3 cells. (A) X-ray microscope image of a cell that was initially living, then rapidly frozen and examined under liquid nitrogen temperatures in the cryostage. No chemical fixatives or contrast enhancement agents were used. Images were obtained using a photon energy of 517 eV ($\lambda = 2.4$ nm), X-ray magnification of 2400×, 0.034 NA, 20 nm pixel size; image size in pixels 2035 × 2033. Note that the image in (A) is a composite of a series of 144 individual X-ray microscope images. (B) One single image showing the first exposure of the edge of a cell nucleus (left) and the 40th exposure of that same region (right) demonstrating the stability of the cryofixed specimen.

fixed (2% paraformaldehyde, 0.1% glutaraldehyde, 100 mM KCl, 3 mM $MgCl_2$, 10 mM HEPES, 150 mM sucrose, 0.1% Triton, pH 7.4, 37 °C, 30 min). Non-specific labelling was blocked with Super Block (SB, Pierce Chemical, Rockford, IL, U.S.A.) in PBS plus 0.1% Triton. Cells were incubated in antibodies recognizing β-tubulin (ICN), rinsed in blocking buffer then incubated in secondary antibodies (FluoroNanogold, Nanoprobes Inc., Yaphank, NY, U.S.A.). After rinsing in PBS they were examined with the confocal microscope. For X-ray microscopy, cells were then post fixed in 2% glutaraldehyde in PBS, rinsed in double distilled H_2O, silver enhanced (Li Ag, Nanoprobes Inc.), rinsed in ddH_2O, then imaged in the hydrated state with the X-ray microscope.

For localization of nuclear pores and splicing factor, cells were permeabilized/extracted for 10 min at room temperature in a cytoskeletal stabilization buffer (CSB; 100 mM NaCl, 300 mM sucrose, 5 mM $MgCl_2$, 10 mM PIPES, pH 6.8) with protease and phosphatase inhibitors (1 mM pefabloc, 10 μg mL^{-1} leupeptin, 10 μg mL^{-1} aprotinin, 10 μg mL^{-1} trypsin inhibitor II, 250 μM NaF, 0.5% Triton), washed in CSB with inhibitors (minus Triton), then fixed (2% paraformaldehyde, 0.1% glutaraldehyde in CSB). Cells were rinsed in PBS, blocked in SB, then incubated in primary antibodies against either nuclear pore complex protein (Mab414, CRP Inc, Richmond, CA, U.S.A.) or splicing factor protein (SRm300) and processed as described above for tubulin.

Results

Cryofixed cells

Mouse 3T3 cells that were rapidly frozen and viewed in a cryostage in the X-ray microscope reveal superior preservation of morphology (Fig. 1A). These cells had not been exposed to any chemical fixatives or contrast enhancement agents, yet fine details of the cell ultrastructure can be seen owing to the striking contrast afforded by X-ray imaging. Numerous organelles, granules of various sizes, and tubular structures (presumably mitochondria) are seen in the cytoplasm. Even the thickest region of the cell – the nucleus (approximately 5 μm thick in these cells) – is easily visualized. Several nucleoli are clearly visible within the nucleus and the surrounding nuclear membrane is sharp and distinct. Cryo transmission X-ray microscopy by the Göttingen group examined specimens frozen by plunge freezing in liquid nitrogen or ethane (Schneider, 1998; Weiss *et al.*, 2000). For the cryo X-ray microscopy shown here, however, we used a unique freezing approach to avoid problems associated with transferring the specimen from the cryogen to specimen stage (which is not under vacuum). The specimen was placed on the microscope stage and frozen using a blast of liquid nitrogen cooled helium gas. The rate of freezing was slower than required to obtain vitreous ice but was sufficient for the level of resolution used to collect these images. It is quite possible, however, that ice crystal damage would be detected in higher magnification views or by examination at higher resolution using electron microscopy. In any event, the frozen cells are extremely stable in the microscope and virtually no detectable change in ultrastructure was observed after 40 consecutive images (Fig. 1B), an accumulative dose of approximately 10^8 Gy. Work of other investigators (i.e. Schneider, 1998) has shown that vitrified samples are stable with dosages up to 10^{10} Gy without degrading the image quality within the resolution limit of the X-ray microscope.

Resolution obtained with the zone plate used to collect this image was 36 nm, as measured with a knife edge (for details, see Materials and methods). The depth of focus with this microscope is on the order of several micrometres; therefore the images shown are two-dimensional projections of three-dimensional data. Further instrumentation will facilitate tomographic reconstructions to restore the three-dimensional information. It has generally been thought that soft X-ray microscopy represented a difficult situation in which the depth of field was too large to provide good optical sectioning and too small to provide images that could be interpreted as projections through the full structure. The solution to this dilemma was thus believed to require a combination of focal-series deconvolution, to build up projections through the full specimen layer-by-layer, followed by tomographic reconstruction from these full projections. There is another approach, however, recently shown by Weiss *et al.* (2000), which demonstrates that using broadband illumination greatly enhances the depth of field and each image can be considered a true projection with no out-of-focus components.

Immunolocalization of cytoplasmic proteins

To identify the subcellular distribution of proteins, we utilized gold-labelled antibodies, which are frequently used for localizing proteins in electron microscopy and, when conjugated with larger gold particles, to identify surface proteins using X-ray microscopy (Schmahl *et al.*, 1994; Yeung *et al.*, 1998). In order to image intracellular proteins with the X-ray microscope we used small (1.4 nm) gold particles, which readily penetrate the Triton-permeabilized plasma membrane of the cell. We then used a silver enhancement technique to increase the gold to a size approximately equal to the resolution of the microscope, a technique routinely used for TEM and recently utilized to image proteins with dark-field scanning transmission X-ray microscopy of dehydrated cells (Chapman *et al.*, 1996). The silver particles are easily identified by the X-ray microscope. For the images reported here the microscope was operated at 517 eV photon energy (2.4 nm wavelength), and photons at this energy readily penetrate the aqueous environment while encountering significant absorption from carbon- and nitrogen-containing organic material or dense metallic particles, such as silver and gold. For X-rays with 517 eV photon energy, the 1/e attenuation lengths of water, organic material and silver are about 10 μm, 0.5 μm and 50 nm, respectively (Henke *et al.*, 1993). Hence, we can clearly distinguish dense, unlabelled cellular structures from the silver-enhanced gold label without contrast enhancement techniques. Figure 2 shows the microtubule network in a whole (fixed but unsectioned), hydrated mouse epithelial cell (EPH4), approximately 8–10 μm thick, imaged with the soft X-ray microscope (XM-1). The microtubule network was labelled using primary antibodies to tubulin followed by gold-conjugated secondary antibodies that were enhanced with silver to form aggregates approximately 50 nm in diameter. Because the direct transmission X-ray microscope image is based on variations in X-ray absorption, we have used a quantitative colour coding approach in which colour corresponds to the degree of absorption. In Fig. 2, blue is indicative of the high density, high absorption silver particles, whereas orange represents less absorbing, organic-rich cell structures. Thus, the microtubule network appears as linear arrays of blue particles coursing throughout the cytoplasm (Fig. 2A). In addition to the microtubules, the unlabelled nucleus and nucleoli are seen as spherical structures, shown here as shades of orange (according to exhibited absorption). The more hydrated (and low absorption) cytoplasmic regions appear dark in

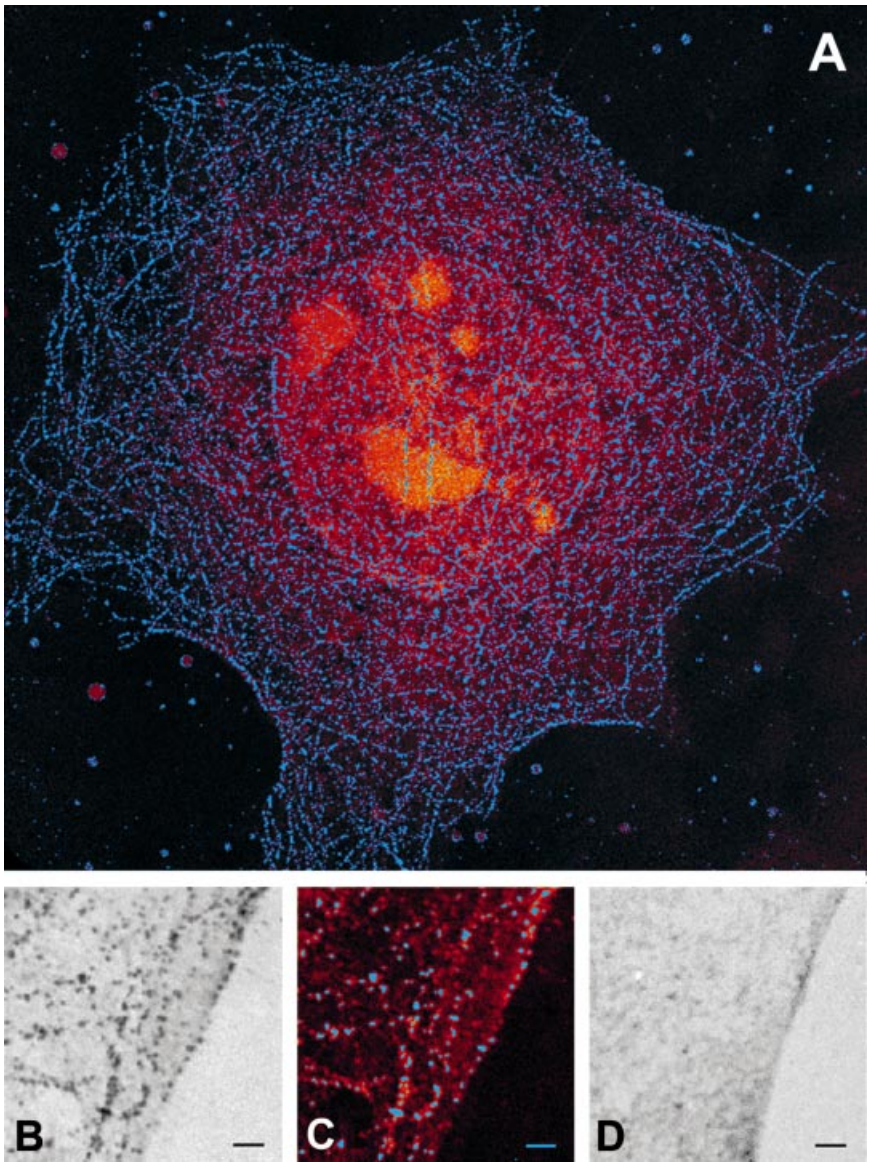

Fig. 2. (A) X-ray microscope image of the labelled microtubule network (blue) in a whole, hydrated mouse mammary epithelial cell (EPH4). The cell nucleus containing several nucleoli (orange) is in the centre of the cell. (B) High magnification view of labelled microtubules before quantitative colour-coding. (C) Same field of view after colour coding of the microtubules with blue. (D) Control cell exposed to gold-conjugated secondary antibodies and silver enhancement (no primary antibody). Images were obtained using a photon energy of 517 eV ($\lambda = 2.4$ nm), X-ray magnification of 2400×, 0.034 NA and 20 nm pixel size; image sizes in pixels. (A) 2035×2033, (B)–(D) 252×252. Note that the image in (A) is a tiled composite of a series of 144 individual, 10 μm × 10 μm, X-ray microscope images.

this image. Higher magnification views of the labelled microtubules (Figs 2B and C) reveal a particulate pattern to the labelling. Although this is unlike the continuous linear microtubules seen with fluorescence microscopy, it is typical of microtubule labelling seen with immunogold electron microscopy and is appropriate for the spatial resolution achieved in these images. The labelling is specific, as demonstrated by the lack of silver particles in control cells not exposed to primary antibodies (Fig. 2D).

Immunolocalization of nuclear proteins

Fine structural details of the nucleus can also be examined using X-ray microscopy of whole cells. Figure 3 illustrates the distribution of nuclear pores on the surface of the nucleus of a human mammary epithelial tumour cell (T4). The nuclear pores were labelled using primary antibodies to a protein from the nuclear pore complex, an elaborate assembly of proteins approximately 45 nm in diameter that span the nuclear membranes of eukaryotic cells and contain an approximately 9 nm opening through which proteins and nucleic acids are transported. The secondary antibody used was conjugated with both fluorescein for detection in the light microscope and 1.4 nm gold particles. This allows us to first examine the cells with the confocal microscope to ensure appropriate labelling (data not shown) then enhance the gold particles with silver and examine the same cells in the X-ray microscope. This image (Fig. 3) reveals a striking view of the distribution of nuclear pores (blue particles,

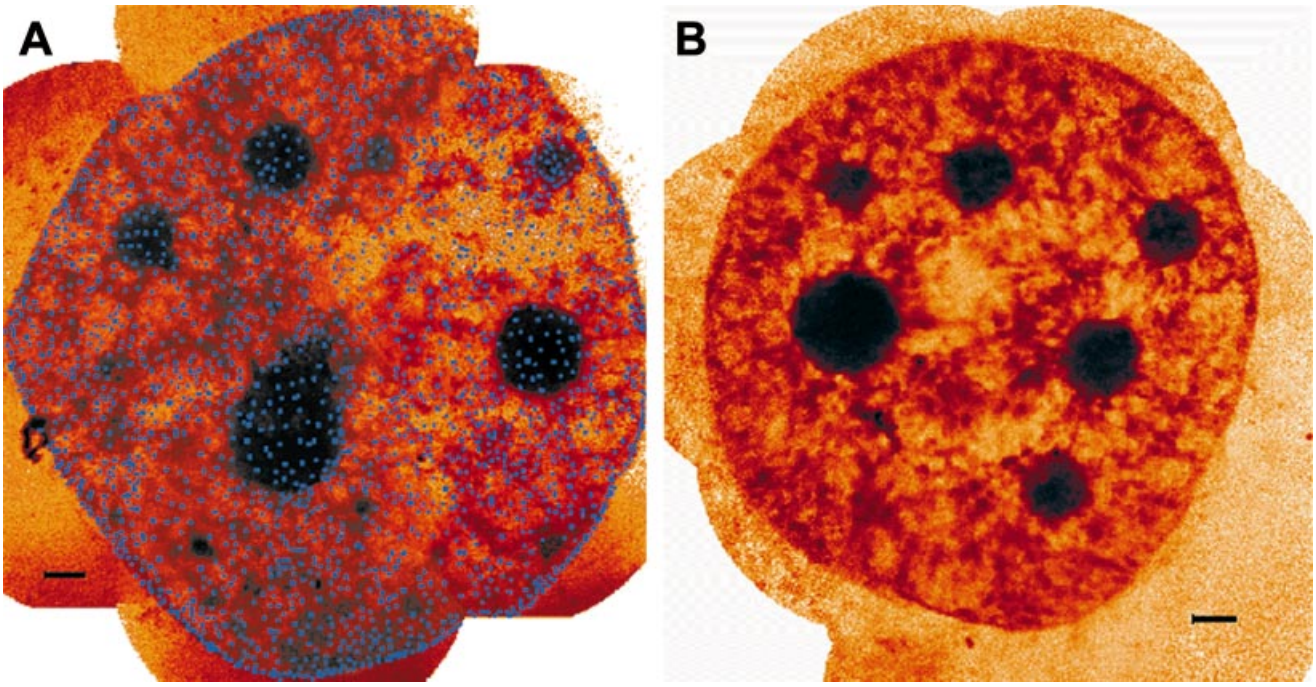

Fig. 3. Nuclei of human mammary epithelial tumour cells (T4) labelled for nuclear pore complex proteins. (A) Colorized X-ray micrograph of a single nucleus after silver enhancement. This image is a montage compiled from four individual X-ray microscope images. (B) Control; single nucleus that was exposed to secondary antibodies and silver enhancement (no primary antibodies). This image is a montage compiled from four individual X-ray microscope images. Magnification = 2400×, 0.034 NA with 20 nm pixel size at 517 eV (λ = 2.4 nm).

Fig. 3) on the surface of the nucleus at better resolution than possible with light microscopy and in a comprehensive view not attainable with the electron microscope.

To demonstrate the ability to examine the distribution of proteins known to be inside the nucleus, we labelled human mammary epithelial tumour cells (T4) with antibodies to a splicing factor, SRm300 (Blencowe *et al.*, 1994). These proteins, which are involved in RNA processing, have been examined using confocal microscopy and electron microscopy (Powell *et al.*, 1997) and shown to be mostly concentrated in clusters, referred to as speckled domains, in the cell nucleus. We show numerous such clusters in an epithelial cell (T4) visualized with silver-enhanced gold in the X-ray microscope (Figs 4A and B). The X-ray micrographs show the clusters of SRm300 splicing factors as dense deposits that are distinct from the unlabelled nucleoli (Fig. 4C) and visualized at a different absorption because of their high concentration of organic material (e.g. RNA and proteins). It has been suggested, based on electron microscopy, that these speckled domains correspond to nuclear structures previously identified as interchromatin granule clusters (Monneron & Bernhard, 1969), which are surrounded by the perichromatin fibrils believed to be the site where splicing occurs (Xing *et al.*, 1995). These structures have engendered a great deal of interest recently because it has been shown that the distribution of RNA splicing factors is dynamic and is modified upon activation of gene expression (Misteli *et al.*, 1997) and cell differentiation (Antoniou *et al.*, 1995; Lelièvre *et al.*, 1998). Soft X-ray microscopy provides a unique method for examining the fine details of such nuclear structures.

Discussion

A combination of cell imaging techniques will be required to analyse the newly identified genes and gene products generated during the genome sequencing era. Modern molecular and structural biology techniques are generating vast amounts of information about molecules *in vitro*. In order to understand their function *in vivo*, however, it is imperative that we also examine these molecules in their natural environment, i.e. in cells. Fluorescent immunocytochemical experiments that examine the location of proteins in cells have provided important insights into protein function and, consequently, have had a considerable impact on our understanding of cell function for several decades. The recent use of light microscopy to track the new, multicoloured, fluorescently tagged proteins, such as GFP constructs (Lippincott-Schwartz *et al.*, 1998; Tsien, 1998; Lippincott-Schwartz *et al.*, 1999; Miller *et al.*, 1999; Larabell, 2000; Taunton *et al.*, 2000), is currently revolutionizing our ability to examine protein function *in vivo*. This technology has enabled studies of the behaviours of specific proteins in living cells as well as their

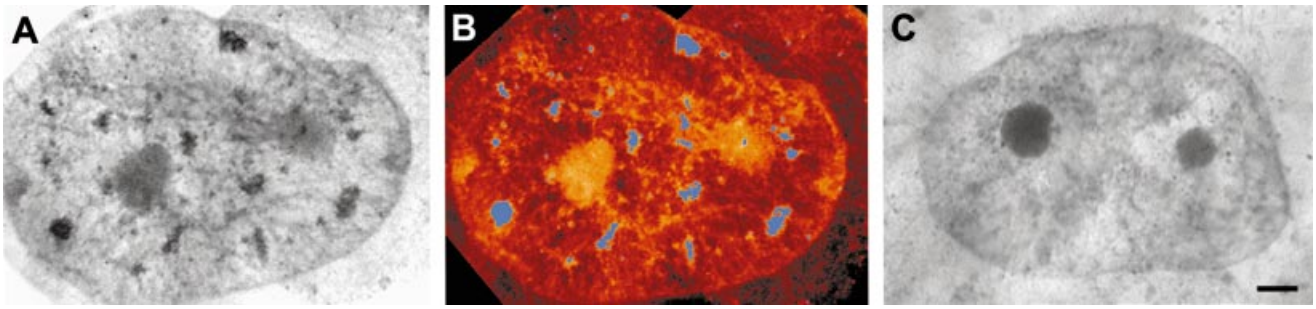

Fig. 4. Nuclei of human mammary epithelial cells (T4) labelled for RNA splicing factor (SRm300). (A) X-ray micrograph of a single nucleus after silver enhancement. This image is a montage compiled from two individual X-ray microscope images. (B) Same nucleus after colour coding to emphasize the label. (C) Control; single nucleus that was exposed to secondary antibodies and silver enhancement but not primary antibodies. This image is a montage compiled from two individual X-ray microscope images. Magnification = 2400×, 0.034 NA with 20 nm pixel size at 517 eV ($\lambda = 2.4$ nm).

reorganization in response to external signals. Fluorescent resonant energy transfer is a powerful technique for examining aspects of short-range (< 5 nm) protein–protein interactions within cells. However, a thorough understanding of the function of these proteins requires information about their precise location in cells at better resolution than is achievable with the light microscope. To date, the use of transmission electron microscopy has been the technique of choice, and the use of immunogold labelling has made this an extremely powerful method (Roth & Heitz, 1989). However, this approach requires elaborate, labour-intensive cell processing procedures and the technique is limited to sectioned or very thin (typically < 1 μm) specimens. Given the parameters of the X-ray microscope used for these studies (XM-1), we can resolve a volume 5–10 times smaller than can be resolved with conventional light microscopy and can obtain information about cell structure and localization of proteins at better than 50 nm resolution. X-ray microscopy can therefore bridge the gap between light and electron microscopy.

Cells that were initially live, then rapidly frozen and examined in the X-ray microscope, demonstrate remarkable structural details about cells that more closely resemble their native state than do chemically fixed cells. Although high voltage electron microscopes can also examine rapidly frozen cells, those microscopes are restricted to examining very thin cells (less than 2–3 μm); in addition, the images obtained are of very low contrast, making ultrastructure details difficult to discern (O'Toole *et al.*, 1993). Soft X-ray microscopy, however, when used to image cells in the 'water window', exploits the strong natural absorptive contrast differences between lipids, proteins, and water to clearly distinguish subcellular components of the cells. The cellular ultrastructure is extremely well preserved and is revealed with a unique combination of high spatial resolution and good contrast, without the need for chemical contrast enhancement agents.

Imaging in the water window also facilitates immunolocalization analyses using silver-enhanced, gold labelling techniques. Using this approach, soft X-ray microscopy can be used to examine the distribution of both cytoplasmic and nuclear proteins at better resolution than is possible with light microscopy. The X-rays have sufficient energy to penetrate thick (up to 10 μm) specimens, eliminating the need for time-consuming sectioning procedures that make it difficult to obtain comprehensive information about protein localizations throughout an entire cell. Not only is serial sectioning an entire cell extremely tedious, but it can also result in loss of information through loss of entire sections or distorted information due to compression of the sections.

The images obtained from the X-ray microscope more closely resemble those obtained from TEM than from light microscopy and therefore the underlying cellular structures to which the labelled antibodies are bound can also be seen. Using this approach, the microtubule networks in the cell cytoplasm, the splicing factors in the nucleus, and the nuclear pore complex proteins in the nuclear envelope were readily identified. The images obtained are, however, two-dimensional projections of three-dimensional data. Stereo tilts and tomography will ultimately restore this three-dimensional data. The feasibility of X-ray tomography has recently been demonstrated by an impressive reconstruction of X-ray microscope images of *Chlamydomonas reinhardtii* that had been examined in a glass capillary tube (Weiss *et al.*, 2000) and of cell monolayers (Wang *et al.*, 2000). X-ray tomography is currently being developed at LBNL for analyses of cultured cells grown in monolayers. This will facilitate analyses of immunolabelled cells that are cryofixed and examined in the cryo-stage followed by tomography to generate three-dimensional information about the localization of proteins throughout the entire cell. In addition, zone plate lenses with better resolution are being developed at the Center for X-ray Optics and are anticipated to generate 10 nm resolution (Carter *et al.*, 1999). Such zone plates will yield excellent three-dimensional views of whole cells, as well as information about the distribution of proteins, at levels of resolution approaching 30 nm. X-ray microscopy

will therefore bridge the existing gap between light and electron microscopy by facilitating analyses of structure-function relationships of molecules in cells.

Acknowledgements

We wish to thank colleagues at the Advanced Light Source, the Center for X-ray Optics, and the Life Sciences Division for their help in this project, in particular M. J. Bissell and D. T. Attwood who have provided both equipment and financial support. We would also like to thank J. A. Nickerson for providing antibodies and for many valuable discussions and comments and B. W. Loo Jr for development of software programs. This work is supported by the Director, Office of Science, Office of Basic Energy Sciences, the Office of Biological and Environmental Research, the Laboratory Directed Research and Development Program of the E. O. Lawrence Berkeley National Laboratory under the Department of Energy contract No. DE-AC03-76SF00098, the National Institutes of Health (Grant CA-64786) to M.J.B., U.S. Army Research Office Grant DAAH04-96-1-0246, U.S. Navy Office of Naval Research, N00014-94-1-0818. Student participation was supported by the Air Force Office of Scientific Research (AFSOR).

References

Antoniou, M., Deboer, E., Spanopoulou, E., Imam, A. & Grosveld, F. (1995) Tbp binding and the rate of transcription initiation from the human beta-globin gene. *Nucl. Acids Res.* **23**, 3473–3480.

Blencowe, B.J., Nickerson, J.A., Issner, R., Penman, S. & Sharp, P.A. (1994) Association of nuclear matrix antigens with exon-containing splicing complexes. *J. Cell Biol.* **127**, 593–607.

Carter, D.J.D., Gil, D., Menon, R., Mondol, M.K., Smith, H.I. & Anderson, E.H. (1999) Maskless, parallel patterning with zone-plate array lithography. *J. Vac. Sci. Technol. B*, **17**, 3449–3452.

Chapman, H.N., Jacobsen, C. & Williams, S. (1996) A characterisation of dark-field imaging of colloidal gold labels in a scanning transmission X-Ray microscope. *Ultramicroscopy*, **62**, 191–213.

Heck, J.M., Meyer-Ilse, W., Anderson, E.H. & Attwood, D.T. (1998) Resolution determination in X-ray microscopy: an analysis of the effects of partial coherence and illumination spectrum. *J. X-Ray Sci. Technol.* **8**, 95–104.

Henke, B.L., Gullikson, E.M. & Davis, J.C. (1993) X–ray interactions – photoabsorption, scattering, transmission, and reflection at E=50–30,000 eV, Z=1–92. *Atom Data Nucl. Data Tables*, **54**, 181–342.

Jacobsen, C. (1999) Soft X-ray microscopy. *Trends Cell Biology*, **9**, 44–47.

Kirz, J., Jacobsen, C. & Howells, M. (1995) Soft X-ray microscopes and their biological applications. *Q. Rev. Biophysics*, **28**, 33–130.

Larabell, C.A. (2000) Confocal microscopy of live *Xenopus* oocytes, eggs, and embryos. *Methods in Molecular Biology*, Vol. 135; *Developmental Biology Protocols, Vol 1*. (ed. by R. S. Tuan and C. W. Lo), pp. 175–182. Humana Press, New Jersey.

Lelièvre, S.A., Weaver, V.M., Nickerson, J.A., Larabell, C.A., Bhaumik, A., Petersen, O.W. & Bissell, M.J. (1998) Tissue phenotype depends on reciprocal interactions between the extracellular matrix and the structural organization of the nucleus. *Proc. Natl. Acad. Sci. USA*, **95**, 14711–14716.

Lippincott-Schwartz, J., Cole, N. & Presley, J. (1998) Unravelling Golgi membrane traffic with green fluorescent protein chimeras. *Trends Cell Biol.* **8**, 16–20.

Lippincott-Schwartz, J., Presley, J.F., Zaal, K.J., Hirschberg, K., Miller, C.D. & Ellenberg, J. (1999) Monitoring the dynamics and mobility of membrane proteins tagged with green fluorescent protein. *Meth. Cell Biol.* **58**, 261–281.

Magowan, C., Brown, J.T., Liang, J., Heck, J., Coppel, R.L., Mohandas, N. & Meyer-Ilse, W. (1997) Intracellular structures of normal and aberrant *Plasmodium falciparum* malaria parasites imaged by soft X-ray microscopy. *Proc. Natl. Acad. Sci. USA*, **94**, 6222–6227.

Methe, O., Spring, H., Guttmann, P., Schneider, G., Rudolph, D., Trendelenburg, M.F. & Schmahl, G. (1997) Transmission X-ray microscopy of intact hydrated PtK2 cells during the cell cycle. *J. Microsc.* **188**, 125–135.

Meyer-Ilse, W., Denbeaux, G., Johnson, L.E., Bates, W., Lucero, A. & Anderson, E.H. (1999) *X-Ray Microscopy VI*. XRM99 (ed. by W. Meyer-Isle, T. Warwick and D. Attwood), pp. 129–134. American Institute of Physics, Melville, New York.

Meyer-Ilse, W., Medecki, H., Jochum, L., Anderson, E., Attwood, D., Magowan, C., Balhorn, R., Moronne, M., Rudolph, D. & Schmahl, G. (1995) New high resolution zone-plate microscope at beamline 6.1 of the ALS. *Synchrotron Radiation News*, **8**, 29–33.

Miller, J.R., Rowning, B.A., Larabell, C.A., Yang-Snyder, J.A., Bates, R.L. & Moon, R.T. (1999) Establishment of the dorsal-ventral axis in *Xenopus* embryos coincides with the dorsal enrichment of Dishevelled that is dependent on cortical rotation. *J. Cell Biol.* **146**, 427–437.

Misteli, T., Caceres, J.F. & Spector, D.L. (1997) The dynamics of a pre-mRNA splicing factor in living cells. *Nature*, **387**, 523–527.

Monneron, A. & Bernhard, W. (1969) Fine structural organization of the interphase nucleus in some mammalian cells. *J. Ultrastruct. Res.* **27**, 266–288.

O'Toole, E., Wray, G., Kremer, J. & McIntosh, J.R. (1993) High voltage cryomicroscopy of human blood platelets. *J. Struct. Biol.* **110**, 55–66.

Powell, R.D., Halsey, C.M.R., Spector, D.L., Kaurin, S.L., McCann, J. & Hainfeld, J.F. (1997) A covalent fluorescent-gold immunoprobe: simultaneous detection of a pre-mRNA splicing factor by light and electron microscopy. *J. Histochem. Cytochem.* **45**, 947–956.

Roth, J. & Heitz, P.U. (1989) Immunolabeling with the protein-A-gold technique – an overview. *Ultrastructural Pathol.* **13**, 467–484.

Scharf, J.G. & Schneider, G. (1999) Ultrastructural characterization of isolated rat Kupffer cells by transmission X-ray microscopy. *J. Microsc.* **193**, 250–256.

Schmahl, G., Guttmann, P., Schneider, G., Niemann, B., David, C., Wilhein, T. & Rudolph, D. (1994) *Phase Contrast Studies of*

Hydrated Specimens with the X-Ray Microscope at BESSY. Bogorodskii Pechatnik Publishing Company, Chernogolovka.

Schmahl, G., Rudolph, D., Niemann, B., Guttmann, P., Thieme, J. & Schneider, G. (1996) *X-Ray microscopy. Naturwissenschaften*, **83**, 61–70.

Schneider, G. (1998) Cryo X-ray microscopy with high spatial resolution in amplitude and phase contrast. *Ultramicroscopy*, **75**, 85–104.

Taunton, J., Rowning, B.A., Coughlin, M.L., Wu, M., Moon, R.T., Mitchison, T.J. & Larabell, C.A. (2000) Actin-dependent propulsion of endosomes and lysosomes by recruitment of N-WASP. *J. Cell Biol.* **148**, 519–530.

Tsien, R.Y. (1998) The green fluorescent protein. *Annu. Rev. Biochem.* **67**, 509–544.

Wang, Y., Jacobsen, C., Maser, J. & Osanna, A. (2000) Soft X-ray microscopy with a cryo scanning transmission X-ray microscope: II. Tomography. *J. Microsc.* **197**, 80–93.

Weiss, D., Schneider, G., Niemann, B., Guttmann, P., Rudolph, D. & Schmahl, G. (2000) Computed tomography of cryogenic biological specimens based on X-ray microscopic images. *Ultramicroscopy*, **84**, 185–197.

Xing, Y.G., Johnson, C.V., Moen, P.T., McNeil, J.A. & Lawrence, J.B. (1995) Nonrandom gene organization – structural arrangements of specific pre-mRNA transcription and splicing with Sc-35 domains. *J. Cell Biol.* **131**, 1635–1647.

Yeung, J., Brown, J.T., Nair, A., Meites, E., Coppel, R.L., Mohandas, N., Meyer-Ilse, W. & Magowan, C. (1998) X-ray microscopic visualization of specific labeling of adhesive molecule CD36 and cytoadherence by *Plasmodium falciparum* infected erythrocytes. *Res. Comms Mol. Pathol. Pharmacol.* **99**, 245–258.

Disclaimer